

## Diffusion as a Probe of the Heterogeneity of Antimicrobial Peptide–Membrane Interactions<sup>†</sup>

Kathryn B. Smith-Dupont,<sup>‡,||</sup> Lin Guo,<sup>§,||</sup> and Feng Gai<sup>\*,§</sup>

<sup>‡</sup>*Department of Biochemistry and Molecular Biophysics and* <sup>§</sup>*Department of Chemistry, University of Pennsylvania, Philadelphia, Pennsylvania 19104* <sup>||</sup>*These authors contributed equally to this work.*

*Received March 20, 2010; Revised Manuscript Received May 6, 2010*

**ABSTRACT:** Many antimicrobial peptides (AMPs) function by forming various oligomeric structures and/or pores upon binding to bacterial membranes. Because such peptide aggregates are capable of inducing membrane thinning and membrane permeabilization, we expected that AMP binding would also affect the diffusivity or mobility of the lipid molecules in the membrane. Herein, we show that measurements of the diffusion times of individual lipids through a confocal volume via fluorescence correlation spectroscopy (FCS) provide a sensitive means of probing the underlying AMP–membrane interactions. In particular, results obtained with two well-studied AMPs, magainin 2 and mastoparan X, and two model membranes indicate that this method is capable of revealing structural information, especially the heterogeneity of the peptide–membrane system, that is otherwise difficult to obtain using common ensemble methods. Moreover, because of the high sensitivity of FCS, this method allows examination of the effect of AMPs on the membrane structure at very low peptide/lipid ratios.

Peptide–membrane interactions play a key role in many biological activities and functions. For example, the innate immune system of many organisms uses antimicrobial peptides (AMPs) as a line of defense against invading bacteria. This arises because the binding and insertion of an AMP can disrupt the structural integrity of the targeted cell membrane (1, 2). Therefore, numerous studies have been devoted to the understanding of the thermodynamics, kinetics, and mechanism of AMP–membrane interactions. Previous studies have provided invaluable insights into the mode of AMP action; however, most of them have drawn their conclusions on the basis of probing certain physical properties of the peptide monomers and oligomers, or the release of a foreign molecule, rather than the lipid (3–7). Thus, it would be advantageous to devise a method that can directly assess the response of the membrane lipids to peptide binding. Herein, we show that the mobility of individual lipid molecules in the membrane provides a sensitive means of monitoring how AMP binding affects the membrane structure, as a previous nuclear magnetic resonance (NMR) study (8) has indicated that the diffusion behaviors of a lipid in a supported bilayer could be significantly altered by the presence of an AMP.

The lateral diffusion of lipids in the membrane system of interest is probed via fluorescence correlation spectroscopy (FCS),<sup>1</sup> which is a commonly used technique for measuring the diffusion time of individual fluorescent molecules through a small confocal volume (9). For a given confocal microscopic setup and solvent condition, the characteristic diffusion time of a diffusing

species is related to its size (9). Thus, FCS has been used to investigate the conformational distribution or heterogeneity of unfolded proteins (10, 11) and lateral organization in model membranes (12–15). Similarly, we expect that FCS can be used to reveal the heterogeneity underlying AMP–membrane interactions. To test this expectation, we use FCS to measure how binding of two well-studied AMPs, magainin 2 (hereafter termed mag2) and mastoparan X (hereafter termed mpX), to model membranes affects the diffusive motion of a small number of fluorescently labeled lipids in the membrane (12, 14, 15).

Mag2 is a 23-amino acid AMP isolated from the African clawed frog, *Xenopus laevis* (16), while mpX is a 14-residue peptide toxin found in the venom of *Vespa xanthoptera* (17). Both peptides are unstructured in aqueous solution but fold into an  $\alpha$ -helical conformation upon association with membranes (18–21). It has been suggested that both peptides disrupt the integrity of the targeted membrane by forming short-lived toroidal pores (3, 4, 18–20). However, depending on the peptide/lipid ratio, the molecularity of the toroidal pores may vary (19, 21–23). In addition, it has been shown that asymmetric binding of these AMPs to a membrane results in local expansion of the headgroup region and thinning of the membrane in the immediate vicinity of the peptide (21, 24–29) and that the orientation and aggregation states of the peptide are determined by local destabilization of the membrane due to the bound peptide/lipid ratio (18, 20, 25, 30, 31). Hence, mag2 and mpX constitute good model systems for testing the aforementioned notion that diffusion measurements could provide useful insight into the mechanism of AMP action, as the latter is expected to modulate the mobility of lipids in the targeted membrane. Indeed, using solid state NMR spectroscopy, Picard et al. have shown that in the presence of a large amount of melittin (peptide/lipid ratio of 1/20) the lateral diffusion of dipalmitoylphosphatidylcholine (DPPC) lipids deposited on silica beads is slowed and the distribution of the diffusion constants is

<sup>†</sup>Supported by the National Institutes of Health (GM-065978) and the National Science Foundation (DMR05-20020).

\*To whom correspondence should be addressed. E-mail: gai@saş.upenn.edu. Phone: (215) 573-6256. Fax: (215) 573-2112.

<sup>1</sup>Abbreviations: FCS, fluorescence correlation spectroscopy; POPC, 1-palmitoyl-2-oleoyl-*sn*-glycero-3-phosphocholine; POPG, 1-palmitoyl-2-oleoyl-*sn*-glycero-3-[phospho-*rac*-(1-glycerol)] (sodium salt); GUV, giant unilamellar vesicle; mag2, magainin 2 amide; mpX, mastoparan X.

broadened (8). Our results further show that the characteristic diffusion times of the lipids in an AMP-bound membrane are distributed over a wide range of time scales, depending on the peptide/lipid ratio, the composition of the membrane, and the sequence of AMP. Taken together, these results not only demonstrate the sensitivity and applicability of the current method in the study of AMP–membrane interactions but also provide new insight into the mechanism of AMP action.

## MATERIALS AND METHODS

**Materials.** All materials were used as received. Fmoc-protected amino acids were purchased from Advanced Chem Tech (Louisville, KY). Mag2 and mpX were synthesized using the standard fluoren-9-ylmethoxycarbonyl (Fmoc)-based solid-phase method on a PS3 peptide synthesizer (Protein Technologies), purified by reverse-phase chromatography, and verified by matrix-assisted laser desorption ionization (MALDI) mass spectroscopy. Phospholipid 1-palmitoyl-2-oleoyl-*sn*-glycero-3-phosphocholine (POPC) and 1-palmitoyl-2-oleoyl-*sn*-glycero-3-[phospho-*rac*-(1-glycerol)] (sodium salt) (POPG) were purchased from Avanti Polar Lipids (Alabaster, AL). Texas Red 1,2-dihexadecanoyl-*sn*-glycero-3-phosphoethanolamine, triethylammonium salt (hereafter termed TR-DHPE), was purchased from Molecular Probes (Eugene, OR).

**Preparation of Giant Unilamellar Vesicles.** Giant unilamellar vesicles (GUVs) were prepared by the standard method of electroswelling (32) using a custom-made closed perfusion chamber and indium–tin oxide (ITO) coated slides (Delta-Technologies, Stillwater, MN) as electrodes. Briefly, 1  $\mu$ mol/mL POPC or a POPC/POPG (3/1 molar ratio) lipid mixture solution was prepared in chloroform. TR-DHPE (0.002%) was then added to the solution; 100 mL of the lipid solution in chloroform was deposited onto an ITO slide. After evaporation of the solvent, the electroswelling chamber was assembled from two lipid-coated ITO slides separated by a rubber spacer and filled with 100 mM sucrose buffer. A voltage of 1.2 V/mm at a frequency of 5 Hz was applied to the system for 2 h while the sample was incubated at 60 °C.

**Sample Preparation for FCS Measurement.** Before each FCS experiment, an aliquot (10  $\mu$ L) of a stock peptide solution at the appropriate concentration (0.2 nM to 20  $\mu$ M) was mixed with an aliquot (10  $\mu$ L) of a GUV suspension to achieve a desired final bulk peptide concentration (0.1 nM to 10  $\mu$ M). Ten microliters of the peptide/GUV solution was then added to a custom-made, closed chamber where the GUVs were allowed to settle for at least 1 h on the bottom of the coverslip. All the FCS traces were collected with GUVs that remained stationary over the course of the experiment. For all the peptide/GUV solutions (containing 25 mM phosphate-buffered saline and 50 mM sucrose buffer), the total lipid concentration is the same. Thus, the peptide/lipid ratio for these solutions is proportional to the peptide concentration. Specifically, the peptide/lipid ratios were estimated to be 1/250000, 1/25000, 1/2500, and 1/250 for the 1 nM, 10 nM, 100 nM, and 1  $\mu$ M peptide solutions, respectively.

**FCS Setup and Data Analysis.** The detail of the FCS apparatus has been described elsewhere (33). In the current study, each FCS curve was obtained by correlating the fluorescence signal for a duration of 40 s. For a given peptide concentration within a set of experiments, more than 250 FCS traces were collected from 25 different GUVs within the apical region of each individual GUV. In addition, all of the FCS curves were carefully

examined and those that were affected by membrane undulations and/or drifting movements were rejected. The remaining FCS autocorrelation curves were fit to the following equation

$$G(\tau) = \left[ \sum_{i=1}^n \frac{1}{N} \left( \frac{f_i}{1 + \frac{\tau}{\tau_D^i}} \right) \right] \left( \frac{1 - T + T e^{-\tau/\tau_{\text{triplet}}}}{1 - T} \right) \quad (1)$$

where  $\tau_D^i$  represents the characteristic diffusion time constant of species  $i$ ,  $N$  represents the number of fluorescent molecules in the confocal volume,  $f_i$  represents the fraction of diffusion component  $i$ ,  $\tau_{\text{triplet}}$  is the triplet lifetime of the fluorophore, and  $T$  represents the corresponding triplet amplitude. It was found that most FCS curves could be adequately fit by a single diffusion component (i.e.,  $n = 1$ ), and only a small number of FCS curves required a second component (i.e.,  $n = 2$ ) to yield a satisfactory fit. For each experimental condition, the resultant  $\tau_D$  values were compiled and presented in a distribution format using a bin size of 200  $\mu$ s.

## RESULTS

To eliminate any potential effects of the coverslip on the diffusion behavior of the lipids in the peptide-bound membranes, we performed all the FCS measurements by placing the focus of the excitation laser beam near the center of the apical region of the GUVs which contain a very small amount of a tracer fluorescently labeled lipid (i.e., 0.002% TR-DHPE). In addition, these GUVs have a diameter of approximately 150  $\mu$ m and remain static and intact on the time scale of the FCS experiments. While occasional thermal fluctuations (13–15, 34) of the lipid bilayer in the confocal volume and movement of the GUV induce additional components in the FCS curve, these motions occur on a time scale much longer than the characteristic diffusion time of the lipids (14) and therefore are not included in the subsequent data analysis and discussion.

**Lipid Diffusion Times in Peptide-Free GUVs.** To determine the effect of AMPs on the mobility of lipid molecules in the membrane of interest, a reference point must be established. Thus, we first measured the characteristic diffusion time (i.e.,  $\tau_D$ ) of the tracer lipid in the membrane of POPC GUVs without the presence of any AMPs. As shown (Figure 1), the diffusion times obtained from repeated measurements are distributed around 1.2 ms (such a distribution is hereafter termed a  $\tau_D$  distribution), which is in agreement with the result of Kahya et al. (14). While this distribution of diffusion times must arise from the heterogeneous environment experienced by individual lipids in the membrane, due likely to transient interactions between lipids (13, 14), its narrow width nevertheless suggests that the degree of heterogeneity in this case is small. As expected (Figure 1), for GUVs consisting of binary mixtures of POPC and POPG (3/1 molar ratio), the diffusion heterogeneity of the tracer lipid is slightly increased.

**Lipid Diffusion Times in mag2-Bound GUVs.** As shown (Figure 2), addition of mag2 to the solution containing POPC/POPG GUVs significantly alters the  $\tau_D$  distribution of the fluorescent tracer lipid. While the variability in GUV samples (e.g., size) could cause the underlying  $\tau_D$  distribution to broaden, the fact that the diffusion times obtained with a single GUV show a broad distribution indicates that the lipid diffusion indeed becomes more heterogeneous in the presence of mag2. It is evident that the shape of the  $\tau_D$  distribution depends on the

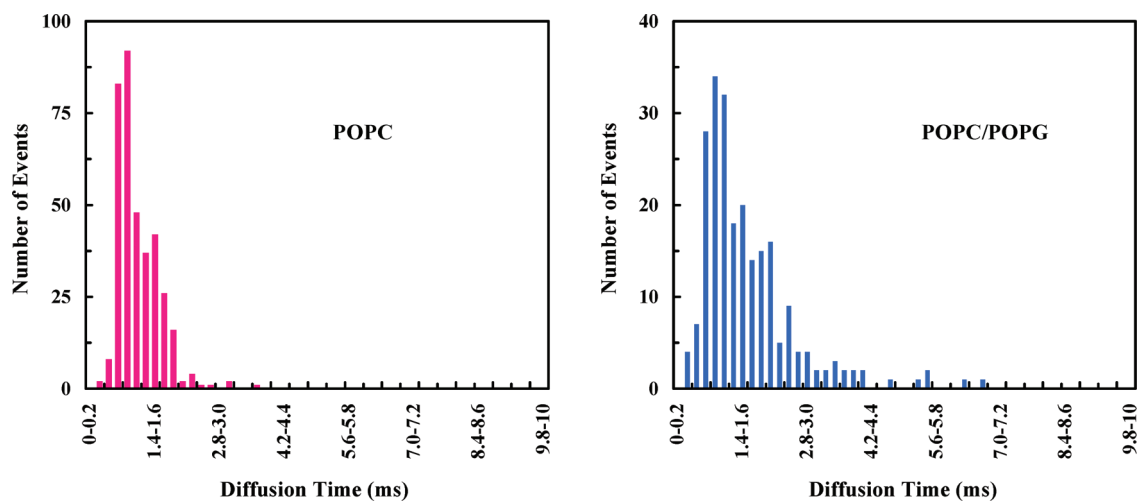


FIGURE 1:  $\tau_D$  distributions of TR-DHPE in POPC or POPC/POPG GUVs, as indicated.

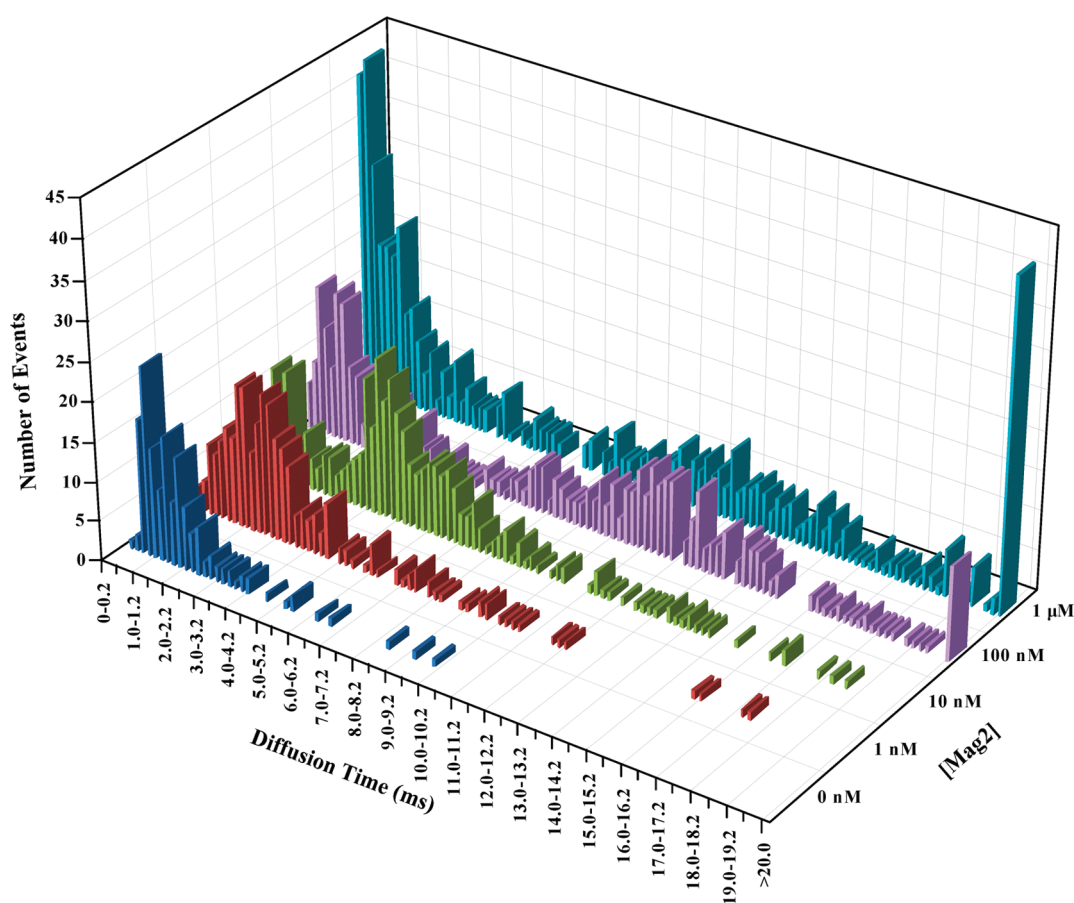


FIGURE 2:  $\tau_D$  distributions of TR-DHPE in POPC/POPG GUVs obtained at different bulk mag2 concentrations, as indicated.

AMP concentration, indicating that measurements of lipid diffusion could provide a convenient yet sensitive means of probing the underlying changes in the membrane structure in response to association with an AMP, even at a very low peptide/lipid ratio. While other studies (19, 21, 22, 24, 25, 27–29, 35–37) have suggested that peptide binding would perturb the lipid dynamics, to the best of our knowledge, the study presented here represents the first systematic investigation of how interaction with an AMP affects the mobility of the lipids in the membrane.

Previous studies have shown that membrane-bound AMPs form transmembrane pores when the bulk peptide/lipid ratio

reaches a critical threshold, which is in the range of 1/300 to 1/10 for mag2, depending on the membrane composition (3, 22). For the GUV samples used in this study, the lipid concentration was estimated to be  $\sim 250 \mu\text{M}$  using a phosphorus assay (38). Thus, for the  $1 \mu\text{M}$  peptide sample, the peptide/lipid ratio was estimated to be approximately 1/250, which is close to the range of critical thresholds reported for mag2 pore formation in POPG bilayers (22). Therefore, those very slow-diffusing species (i.e., those with a  $\tau_D$  of  $\geq 20$  ms) observed at a peptide concentration of  $1 \mu\text{M}$  could be attributed to (transient) pore formation. Nevertheless, it is apparent that even at very low

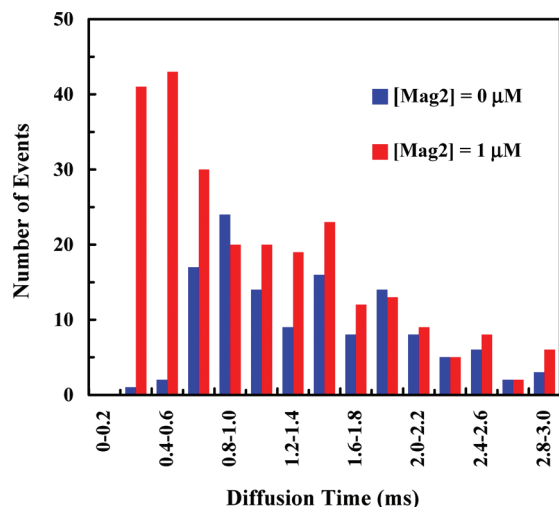


FIGURE 3: Comparison of the  $\tau_D$  distributions of TR-DHPE in POPC/POPG GUVs obtained with and without mag2.

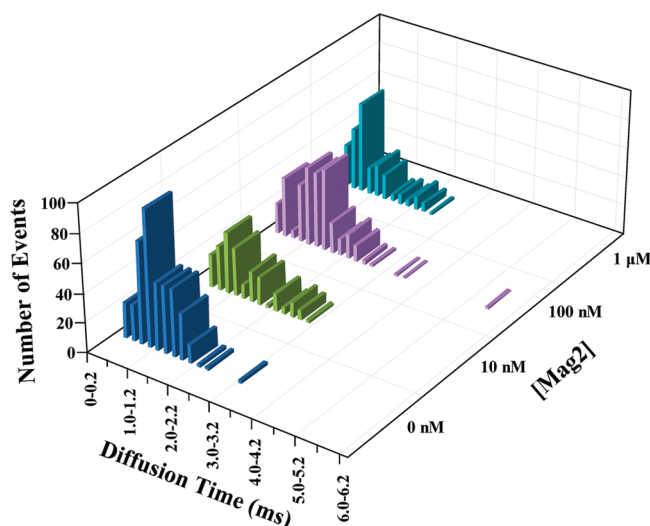


FIGURE 4:  $\tau_D$  distributions of TR-DHPE in POPC GUVs obtained at different bulk mag2 concentrations, as indicated.

peptide concentrations (e.g., 1 and 10 nM), in which no pores are expected to form, the corresponding  $\tau_D$  distributions are drastically different from that measured in the absence of mag2, suggesting that pore formation is not the main underlying cause of the decrease in lipid mobility. In addition, results obtained at relatively high concentrations of mag2 (i.e., 100 nM and 1  $\mu$ M) clearly show that some lipids even diffuse faster than those in the unperturbed GUV membranes (Figure 3).

Since the activity of AMPs depends on the membrane composition (5), we further studied how mag2 affects the mobility of lipids in GUVs composed of POPC. As shown (Figure 4), the resultant  $\tau_D$  distributions are less heterogeneous in comparison to those obtained with POPC/POPG GUVs, consistent with the fact that mag2 has a weaker affinity for zwitterionic membranes (5, 39).

**Lipid Diffusion Times in mpX-Bound GUVs.** To further substantiate the notion that lipid diffusion is a useful probe of AMP–membrane interactions, we also measured the  $\tau_D$  distributions of the tracer fluorescent lipid in both POPC and POPC/POPG GUVs in the presence of another AMP, mpX. As expected, binding of mpX to these model membranes also causes the  $\tau_D$  distribution to broaden (Figures 5 and 6). Compared to

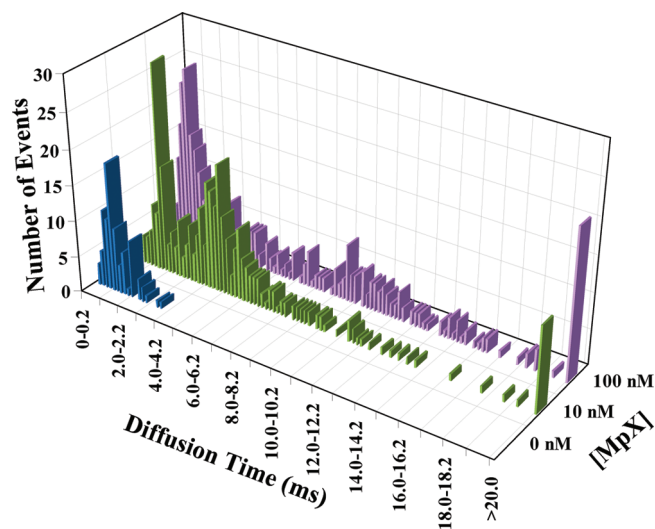


FIGURE 5:  $\tau_D$  distributions of TR-DHPE in POPC/POPG GUVs obtained at different bulk mpX concentrations, as indicated.

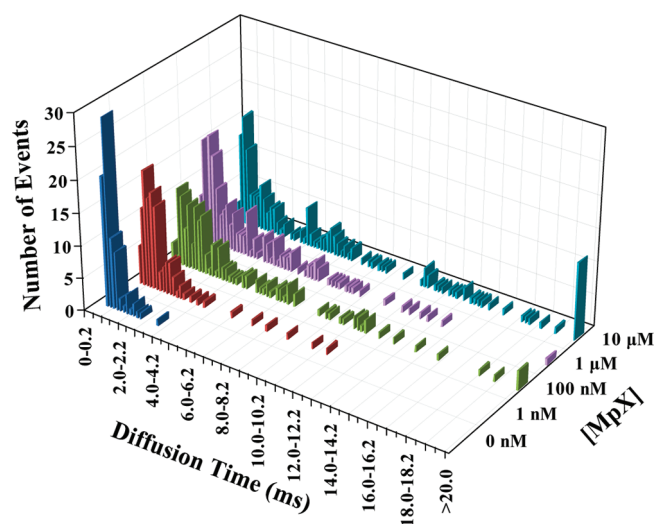


FIGURE 6:  $\tau_D$  distributions of TR-DHPE in POPC GUVs obtained at different bulk mpX concentrations, as indicated.

those obtained with mag2, however, the effects of mpX on the lipid mobility are clearly different. For example, even at a mpX concentration of 10  $\mu$ M, the very fast-diffusing species observed in the case of mag2 is not present (Figure 7). Thus, these results further demonstrate the sensitivity of the current method.

## DISCUSSION

Because of their biological significance, the AMP–membrane interactions have been the subject of extensive studies. However, most ensemble methods employed in previous studies are unable to reveal the intrinsic heterogeneity associated with such interactions and also lack the ability to probe the perturbation to the membrane structure at low peptide/lipid ratios. On the other hand, techniques based on FCS, which is able to measure lipid dynamics in GUVs at the pseudo-single-molecule level (12–15), are suitable for revealing the effect of AMPs on membranes that might be difficult to determine by other methods. Herein, we show that the mobility of the lipid molecules is a sensitive probe of the effect of AMPs on the structural integrity of the targeted membrane for a wide range of peptide/lipid ratios.

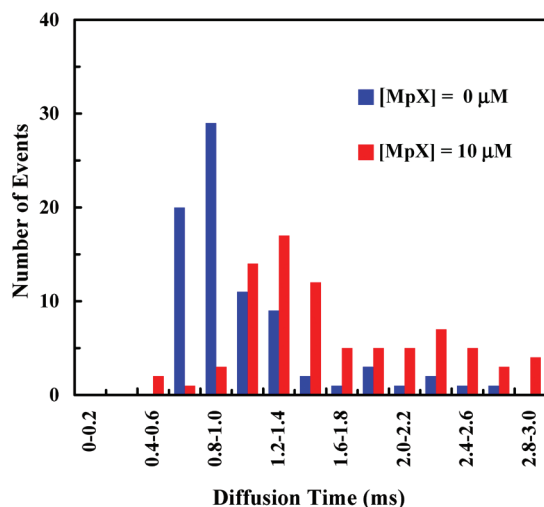


FIGURE 7: Comparison of the  $\tau_D$  distributions of TR-DHPE in POPC GUVs obtained with and without mpX.

**Effect of Peptide Concentration.** Previous studies have shown that the activity of mag2 and mpX depends on the local peptide concentration in the membrane (23). Huang and co-workers (30) have proposed a two-state-like model to understand this dependence in which the S state, which is inactive, is populated at relatively low peptide concentrations. While it is generally believed that in the S state the peptides form monomeric  $\alpha$ -helices and lie on the surface of the membrane (30), it has been difficult to characterize the changes in the membrane structure induced by adsorption of a relatively small number of peptides. For both mag2 and mpX, our results show that even in the S state these peptides can induce significant changes in the diffusion dynamics and hence the packing of the lipids.

Recently, a vesicle fluctuation analysis study (27) indicated that the membrane bending rigidity of POPC GUVs decreases drastically upon interaction with mag2, even at a very low peptide surface coverage. Consistent with this picture, our results show that at 1 nM mag2 (Figure 2), where the bulk peptide/lipid ratio is estimated to be approximately 1/250000, the  $\tau_D$  distribution of TR-DHPE obtained in POPC/POPG GUVs is noticeably different from that obtained in the absence of any peptides, with the appearance of slower-diffusing species. As expected, increasing the peptide concentration increases the population of the lipids whose diffusion dynamics are affected. The latter is evidenced by the appearance of separate peaks in the  $\tau_D$  distribution, as well as the increased width of the distribution. Under the current experimental conditions, mag2 and mpX are not expected to induce any micellization or disintegration of the GUVs (40), which was confirmed by visual inspection of the GUVs through a microscope eyepiece. Thus, the resulting distributions in  $\tau_D$  manifest peptide-induced structural and/or organizational changes in the membrane instead of membrane destruction. Consistent with this picture, a recent molecular dynamics (MD) simulation study (41) showed that asymmetric binding of a related AMP, magainin H2, to a DPPC lipid bilayer creates a local tension in the membrane and asymmetric perturbation of the lipid order.

However, achieving a quantitative interpretation of such  $\tau_D$  distributions is difficult, as they present a “chaotic-like” picture regarding the AMP–membrane interactions, especially those obtained at relatively high peptide concentrations. For example, the  $\tau_D$  distributions obtained at 100 nM and 1  $\mu$ M mag2 are

exceedingly broad and consist of several peaks (Figure 2). Since the diffusivity of a membrane species (i.e., lipid or lipid-solvated peptide monomer or oligomer in the current case) depends on several factors (42, 43), there are two possible interpretations for why the diffusion time of the tracer lipids shows a distribution. First, the decreased lipid diffusion time in AMP-bound membranes could be due to the formation of stable or transient peptide–lipid clusters. It is known that membrane-bound AMPs can form various peptide species (18, 44–46), such as monomer, dimer, oligomer, and transient or stable pores. Thus, it is probable that some lipids that are “solvating” such peptide species could diffuse together with the peptide species and, as a result, show a decrease in their mobility because of an increase in their effective size (i.e., the size that determines the diffusion coefficient of the peptide–lipid cluster). In this case, the widespread distribution of the diffusion times is a direct manifestation of the existence of a large number of stable or transient peptide–lipid clusters of different sizes. While this interpretation is to some extent attractive, it has limitations.

Theoretical treatments of two-dimensional diffusion in membranes based on both the free volume and continuum models are available (42, 43). For example, Saffman and Delbrück (47) have shown that the diffusion coefficient of a transmembrane-bound protein is proportional to the logarithm of the reciprocal of its radius. While the applicability of the Saffman and Delbrück (SD) model has been shown to have a size limit (48), we used it to estimate the sizes of the slow-diffusing species observed in our case with the assumption that the diffusing entity corresponds to a cluster formed by lipid and peptide molecules. On the basis of the SD relationship measured by Ramadurai et al. (49), a diffusing object that has a diffusion time of 4 ms (12 ms) in our case would have an effective radius of  $\sim 7.0$  nm (75 nm). While forming tightly packed peptide–lipid clusters of 7 nm is entirely possible (50), it seems unlikely that a peptide species can recruit enough lipids to form a tightly packed cluster as large as 75 nm. Furthermore, the size of the pores formed by mag2 has been estimated to be approximately 2–5 nm, containing four to seven peptides and approximately 90 lipid molecules (2, 20). Thus, on the basis of the SD model, even those lipids that are trapped in the lining of a peptide pore and thus move together with the pore are expected to have a diffusion time of less than 4 ms. Taken together, these pieces of evidence suggest that we cannot simply attribute the observed  $\tau_D$  distribution to the formation of oligomeric peptide species.

The second possibility is that the widespread distribution of lipid diffusion times does not reflect, at least not directly, the size distribution of peptide–lipid species or clusters. Instead, it is a manifestation of AMP-induced perturbations to the local lipid organizations or peptide-induced membrane domain formation (or long-range correlations between lipids). Domain formation has been recently proposed as an alternative mechanism of action for certain antimicrobial peptides, including mag2 (5, 29, 51–58). Using fluorescence microscopy, Oreopoulos et al. have shown that AMP-induced domains in supported lipid bilayers can have very different sizes, ranging from diffraction-limited to micrometer-sized (59), which is in accordance with our observation that in AMP-bound membranes the diffusion times of the labeled lipids are distributed over a wide range of time scales. In addition, our observation is consistent with the study of Bacia et al. (13), which showed that the diffusion times of a probe lipid in lipid-ordered and lipid-disordered domains can differ by an order of magnitude.

Interestingly, the  $\tau_D$  distributions obtained at mag2 concentrations of 100 nM and 1  $\mu$ M in both types of lipid membranes clearly show the presence of a diffusion component centered at  $\sim 400$   $\mu$ s (Figure 3), which is faster than the mean diffusion time ( $\sim 1$  ms) of the lipids in peptide-free membranes. Since this component is absent in the  $\tau_D$  distributions obtained at lower peptide concentrations, it most likely arises from the sequestration of lipids due to peptide oligomerization and/or transient pore formation, leaving loosely packed regions of lipid molecules in the membrane. This picture is consistent with the notion that AMPs can induce membrane thinning and softening (21, 27, 48–50), resulting in an increase in the lateral surface area per lipid and also a decrease in the membrane's bending rigidity (21, 27, 50).

**Effect of Membrane Composition.** It is known that the chemical and physical properties of the lipids play an important role in determining the structure and dynamics of membranes and peptide–membrane interactions. For example, many AMPs, including mag2 and mpX, interact more favorably with anionic membranes rather than zwitterionic membranes (38). Indeed, diffusion measurements indicate that the effect of AMPs on the mobility of the lipids in POPC membranes is different from that of POPC/POPG membranes (Figures 2–7). It is apparent that at the same bulk peptide concentration, the structure of the POPC membranes is less perturbed upon peptide binding. This is consistent with the fact that mag2 exhibits a  $> 100$ -fold weaker binding affinity toward POPC membranes (6, 60, 61) and that electrostatic forces are important for AMP–membrane interactions (23, 39, 62). In addition, the stronger effect of both mag2 and mpX on POPC/POPG or negatively charged membranes corroborates the aforementioned hypothesis that the observed  $\tau_D$  distribution largely reflects domain formation, as it has been shown that cationic antimicrobial agents exhibit a stronger effect on domain formation for membranes consisting of both zwitterionic and anionic lipids than for zwitterionic membranes (63) and that binding of a cationic AMP induces a greater reduction in the packing order of the acyl chains in anionic membranes than in zwitterionic membranes (64).

**Effect of AMPs.** To show that the peptide-induced lipid mobility change is not specific to mag2, we repeated all of the experiments with mpX. As indicated (Figure 5), binding of mpX to POPC/POPG membranes induces a change in the mobility of the lipid that is qualitatively similar to that observed for mag2 (Figure 2). However, the  $\tau_D$  distributions obtained with these two peptides also show significant differences. For example, for mpX, even at the highest peptide concentration studied, the very fast diffusion component ( $\sim 400$   $\mu$ s) observed for mag2 is not observed. This is likely due to the smaller size of mpX and also the smaller number of positive charges it carries. In addition, it is apparent that mpX has a stronger effect on the diffusivity of lipids in POPC membranes than mag2 (Figures 4 and 6), due presumably to the fact that mpX has a stronger binding affinity than mag2 toward POPC membranes (60, 61).

In summary, the diffusion data obtained with both mag2 and mpX indicate that FCS is a versatile technique for studying AMP-induced structural changes of the targeted membrane over a wide range of peptide/lipid ratios and could be used to screen AMPs. In addition, these data indicate that, from a lipid perspective, even a relatively small number of membrane-bound peptides can induce noticeable changes in the membrane structure. While further experimental and theoretical studies are needed to establish the relation between lipid diffusivity and AMP activity, the continuous increase in the width and

complexity of the  $\tau_D$  distribution with an increasing peptide concentration seems to suggest that models that go beyond the “all-or-nothing” framework (5) should be considered. Furthermore, to facilitate a more comprehensive and quantitative understanding of these results, measurements of AMP diffusivity at different peptide/lipid ratios are also needed.

## CONCLUSIONS

We demonstrate in this study that the diffusivity of lipids in an AMP-bound membrane is a useful probe of the AMP-induced structural changes of the membrane. For both magainin 2 and mastoparan X, our results show that peptide binding can significantly alter the diffusion time ( $\tau_D$ ) of individual lipids in the membrane through a small confocal volume, measured via fluorescence correlation spectroscopy (FCS). In particular, we found that the lipid diffusion times obtained from repeated measurements under the same experimental conditions are distributed over a wide range of time scales, and that the characteristics of the resultant  $\tau_D$  distribution depend on the peptide/lipid ratio, the AMP sequence, and the membrane composition, which demonstrates the sensitivity and also applicability of the current method. In addition, the observed heterogeneity in lipid diffusion is attributed to AMP-induced domain formation, an aspect that has been shown to be important to AMP activities.

## REFERENCES

- Dathe, M., and Wieprecht, T. (1999) Structural features of helical antimicrobial peptides: Their potential to modulate activity on model membranes and biological cells. *Biochim. Biophys. Acta* 1462, 71–87.
- Sato, H., and Feix, J. B. (2006) Peptide-membrane interactions and mechanisms of membrane destruction by amphipathic  $\alpha$ -helical antimicrobial peptides. *Biochim. Biophys. Acta* 1758, 1245–1256.
- Matsuzaki, K., Murase, O., and Miyahjima, K. (1995) Kinetics of pore formation by an antimicrobial peptide, magainin 2, in phospholipid bilayers. *Biochemistry* 34, 12553–12559.
- Matsuzaki, K., Yoneyama, S., Murase, O., and Miyahima, K. (1996) Transbilayer transport of ions and lipids coupled with mastoparan X translocation. *Biochemistry* 35, 8450–8456.
- Gregory, S. M., Pokorny, A., and Almeida, P. F. F. (2009) Magainin 2 revisited: A test of the quantitative model for the all-or-none permeabilization of phospholipid vesicles. *Biophys. J.* 96, 116–131.
- Matsuzaki, K., Harada, M., Handa, T., Funakoshi, S., Fujii, N., Yajima, H., and Miyajima, K. (1989) Magainin 1-induced leakage of entrapped calcein out of negatively-charged lipid vesicles. *Biochim. Biophys. Acta* 981, 130–134.
- Duclohier, H., Molle, G., and Spach, G. (1989) Antimicrobial peptide magainin 1 from *Xenopus* skin forms anion-permeable channels in planar lipid bilayers. *Biophys. J.* 56, 1017–1021.
- Picard, F., Paquet, M.-J., Dufourc, E. J., and Auger, M. (1998) Measurement of the lateral diffusion of dipalmitoylphosphatidylcholine adsorbed on silica beads in the absence and presence of melittin: A  $^{31}$ P two-dimensional exchange solid-state NMR study. *Biophys. J.* 74, 857–868.
- Magde, D., Elson, E. L., and Webb, W. W. (1974) Fluorescence correlation spectroscopy. 2. Experimental realization. *Biopolymers* 13, 29–61.
- Sherman, E., Itkin, A., Kuttner, Y. Y., Rhoades, E., Amir, D., Haas, H., and Haran, G. (2008) Using fluorescence correlation spectroscopy to study conformational changes in denatured proteins. *Biophys. J.* 94, 4819–4827.
- Guo, L., Chowdhury, P., Glasscock, J. M., and Gai, F. (2008) Denaturant-induced expansion and compaction of a multi-domain protein: IgG. *J. Mol. Biol.* 384, 1029–1036.
- Chiantia, S., Ries, J., and Schwill, P. (2009) Fluorescence correlation spectroscopy in membrane structure elucidation. *Biochim. Biophys. Acta* 1788, 225–233.
- Bacia, K., Scherfeld, D., Kahya, N., and Schwill, P. (2004) Fluorescence correlation spectroscopy relates rafts in model and native membranes. *Biophys. J.* 87, 1034–1043.
- Kahya, N., and Schwill, P. (2006) Fluorescence correlation studies of lipid domains in model membranes. *Mol. Membr. Biol.* 23, 29–39.

15. Chen, Y., Lagerholm, B. C., Yang, B., and Jacobson, K. (2006) Methods to measure the lateral diffusion of membrane lipids and proteins. *Methods* 39, 147–153.
16. Zasloff, M. (1987) Magainins, a class of antimicrobial peptides from *Xenopus* skin: Isolation, characterization of 2 active forms, and partial cDNA sequence of a precursor. *Proc. Natl. Acad. Sci. U.S.A.* 84, 5449–5453.
17. Hirai, Y., Kuwada, M., Yasuhara, T., Yoshida, H., and Nakajima, T. (1979) New mast-cell degranulating peptide homologous to mastoparan in the venom of Japanese hornet (*Vespa xanthoptera*). *Chem. Pharm. Bull.* 27, 1945–1946.
18. Matsuzaki, K., Murase, O., Tokuda, H., Funakoshi, S., Fujii, N., and Miyajima, K. (1994) Orientational and aggregational states of magainin 2 in phospholipid bilayers. *Biochemistry* 33, 3342–3349.
19. Matsuzaki, K., Murase, O., Fujii, N., and Miyajima, K. (1996) An antimicrobial peptide, magainin 2, induced rapid flip-flop of phospholipids coupled with pore formation and peptide translocation. *Biochemistry* 35, 11361–11368.
20. Ludtke, S. J., He, K., Heller, W. T., Harroun, T. A., Yang, L., and Huang, H. W. (1996) Membrane pores induced by magainin. *Biochemistry* 35, 13723–13728.
21. Ludtke, S., He, K., and Huang, H. (1995) Membrane thinning caused by magainin 2. *Biochemistry* 34, 16764–16769.
22. Matsuzaki, K., Sugishita, K.-I., Ishibe, N., Uehna, M., Nakata, S., Miyajima, K., and Eppard, R. M. (1998) Relationship of membrane curvature to the formation of pores by magainin 2. *Biochemistry* 37, 11856–11863.
23. Tamba, Y., and Yamazaki, M. (2009) Magainin 2-induced pore formation in the lipid membranes depends on its concentration in the membrane interface. *J. Phys. Chem. B* 113, 4846–4852.
24. Zhao, H., Mattila, J.-P., Holopainen, J. M., and Kinnunen, P. K. J. (2001) Comparison of the membrane association of two antimicrobial peptides, magainin 2 and indolicidin. *Biophys. J.* 81, 2979–2991.
25. Lee, M.-T., Hung, W.-C., Chen, F.-Y., and Huang, H. W. (2005) Many-body effect of antimicrobial peptides: On the correlation between lipid's spontaneous curvature and pore formation. *Biophys. J.* 89, 4006–4016.
26. Lee, M.-T., Hung, W.-C., Chen, F.-Y., and Huang, H. W. (2008) Mechanism and kinetics of pore formation in membranes by water-soluble amphipathic peptides. *Proc. Natl. Acad. Sci. U.S.A.* 105, 5087–5092.
27. Bouvrais, H., Meleard, P., Pott, T., Jensen, K. J., Brask, J., and Ipsen, J. H. (2008) Softening of POPC membranes by magainin. *Biophys. Chem.* 137, 7–12.
28. Khandelia, H., Ipsen, J. H., and Mouritsen, O. G. (2008) The impact of peptides on lipid membranes. *Biochim. Biophys. Acta* 1778, 1528–1536.
29. Salnikov, E. S., Mason, A. J., and Bechinger, B. (2009) Membrane order perturbation in the presence of antimicrobial peptides by H-2 solid-state NMR spectroscopy. *Biochimie* 91, 734–743.
30. Huang, H. W. (2000) Action of antimicrobial peptides: Two-state model. *Biochemistry* 39, 8347–8352.
31. Huang, H. W. (2009) Free energies of molecular bound states in lipid bilayers: Lethal concentrations of antimicrobial peptides. *Biophys. J.* 96, 3263–3272.
32. Mathivet, F., Cribrier, S., and Devaux, P. F. (1996) Shape change and physical properties of giant phospholipid vesicles prepared in the presence of an AC electric field. *Biophys. J.* 70, 1112–1121.
33. Chowdhury, P., Wang, W., Lavender, S., Bunagan, M. R., Klemke, J. W., Tang, J., Saven, J. G., Cooperman, B. S., and Gai, F. (2007) Fluorescence Correlation Spectroscopic Study of Serpin Depolymerization by Computationally Designed Peptides. *J. Mol. Biol.* 369, 462–473.
34. Milon, S., Hovius, R., Vogel, H., and Wohland, T. (2003) Factors influencing fluorescence correlation spectroscopy measurements on membranes: Simulations and experiments. *Chem. Phys.* 288, 171–186.
35. Wierprecht, T., Beyermann, M., and Seelig, J. (1999) Binding of antibacterial magainin peptides to electrically neutral membranes: Thermodynamics and structure. *Biochemistry* 38, 10377–10387.
36. Munster, C., Spaar, A., Bechinger, B., and Salditt, T. (2002) Magainin 2 in phospholipid bilayers: Peptide orientation and lipid chain ordering studied by X-ray diffraction. *Biochim. Biophys. Acta* 1562, 37–44.
37. Hallock, K. J., Lee, D. K., and Ramamoorthy, A. (2003) MSI-78, an analogue of the magainin antimicrobial peptides, disrupts lipid bilayer structure via positive curvature strain. *Biophys. J.* 84, 3052–3060.
38. Bartlett, G. R. (1959) Phosphorus assay in column chromatography. *J. Biol. Chem.* 234, 466–468.
39. Wierprecht, T., Dathe, M., Eppard, R. M., Beyermann, M., Krause, E., Maloy, W. L., MacDonald, D. L., and Bienert, M. (1997) Influence of the angle subtended by the positively charged helix face on the membrane activity of amphipathic, antibacterial peptides. *Biochemistry* 36, 12869–12880.
40. Tamba, Y., and Yamazaki, M. (2005) Single giant unilamellar vesicle method reveals effect of antimicrobial peptide magainin 2 on membrane permeability. *Biochemistry* 44, 15823–15833.
41. Leontiadou, H., Mark, A. E., and Marrink, S. J. (2006) Antimicrobial peptides in action. *J. Am. Chem. Soc.* 128, 12156–12161.
42. Vaz, W. L. C., Clegg, R. M., and Hallmann, D. (1985) Translational diffusion of lipids in liquid crystalline phase phosphatidylcholine multibilayers. A comparison of experiment with theory. *Biochemistry* 24, 781–786.
43. Liu, C., Paprica, A., and Petersen, N. O. (1997) Effects of size of macrocyclic polyamides on their rate of diffusion in model membranes. *Biophys. J.* 73, 2580–2587.
44. Schumann, M., Dathe, M., Wierprecht, T., Beyermann, M., and Bienert, M. (1997) The tendency of magainin to associate upon binding to phospholipid bilayers. *Biochemistry* 36, 4345–4351.
45. Hara, T., Kodama, H., Kondo, M., Wakamatu, K., Takeda, A., Tachi, T., and Matsuzaki, M. (2001) Effects of peptide dimerization on pore formation: Antiparallel disulfide-dimerized magainin 2 analogue. *Biopolymers* 58, 437–446.
46. Matsuzaki, K. (1999) Why and how are peptide-lipid interactions utilized for self-defense? Magainins and tachyplesins and archetypes. *Biochim. Biophys. Acta* 1462, 1–10.
47. Saffman, P. G., and Delbrück, M. (1975) Brownian motion in biological membranes. *Proc. Natl. Acad. Sci. U.S.A.* 72, 3111–3113.
48. Guigas, G., and Weiss, M. (2006) Size-dependent diffusion of membrane inclusions. *Biophys. J.* 91, 2393–2398.
49. Ramadurai, S., Holt, A., Krasnikov, V., van den Bogaart, G., Killian, J. A., and Poolman, B. (2009) Lateral diffusion of membrane proteins. *J. Am. Chem. Soc.* 131, 12650–12656.
50. Zemel, A., Ben-Shaul, A., and May, S. (2004) Membrane perturbation induced by interfacially adsorbed peptides. *Biophys. J.* 86, 3607–3619.
51. Pabst, G., Danner, S., Podgornik, R., and Katsaras, J. (2007) Entropy-driven softening of fluid lipid bilayers by alamethicin. *Langmuir* 23, 11705–11711.
52. Eppard, R. F., Schmitt, M. A., and Eppard, R. M. (2006) Role of membrane lipids in the mechanism of bacterial species selective toxicity by two  $\alpha/\beta$ -antimicrobial peptides. *Biochim. Biophys. Acta* 1758, 1343–1350.
53. Mason, A. J., Marquette, A., and Bechinger, B. (2007) Zwitterionic phospholipids and sterols modulate antimicrobial peptide-induced membrane destabilization. *Biophys. J.* 93, 4289–4299.
54. Jean-François, F., Castano, S., Desbat, B., Odaert, B., Roux, M., Metz-Boutigue, M.-H., and Dufour, E. J. (2008) Aggregation of cateslytin  $\beta$ -sheets on negatively charged lipids promotes rigid membrane domains. A new mode of action for antimicrobial peptides? *Biochemistry* 47, 6394–6402.
55. Arouri, A., Dathe, M., and Blume, A. (2009) Peptide induced demixing in PG/PE lipid mixtures: A mechanism for the specificity of antimicrobial peptides towards bacterial membranes? *Biochim. Biophys. Acta* 1788, 650–659.
56. Joanne, P., Galanth, C., and Alves, I. D. (2009) Lipid reorganization induced by membrane-active peptides probed using differential scanning calorimetry. *Biochim. Biophys. Acta* 1788, 1772–1781.
57. Eppard, R. M., and Eppard, R. F. (2009) Domains in bacterial membranes and the action of antimicrobial agents. *Mol. Biosyst.* 5, 580–587.
58. Eppard, R. M., and Eppard, R. F. (2009) Lipid domains in bacterial membranes and the action of antimicrobial agents. *Biochim. Biophys. Acta* 1788, 289–294.
59. Oreopoulos, J., Eppard, R. F., Eppard, R. M., and Yip, C. M. (2010) Peptide-induced domain formation in supported lipid bilayers: Direct evidence by combined atomic force and polarized total internal reflection fluorescence microscopy. *Biophys. J.* 98, 815–823.
60. Almeida, P. F., and Pokorny, A. (2009) Mechanisms of antimicrobial, cytolytic, and cell-penetrating peptides: From kinetics to thermodynamics. *Biochemistry* 48, 8083–8093.
61. Yandek, L. E., Pokorny, A., and Almeida, P. F. F. (2009) Wasp mastoparans follow the same mechanism as the cell-penetrating peptide transportan 10. *Biochemistry* 48, 7342–7351.
62. Matsuzaki, K., Sugishita, K., Harada, M., Fujii, N., and Miyajima, K. (1997) Interactions of an antimicrobial peptide, magainin 2, with outer and inner membranes of Gram-negative bacteria. *Biochim. Biophys. Acta* 1327, 119–130.
63. Eppard, R. M., Rotem, S., Mor, A., Berno, B., and Eppard, R. F. (2008) Bacterial membranes as predictors of antimicrobial potency. *J. Am. Chem. Soc.* 130, 14346–14352.
64. Mason, A. J., Chotimah, I. N. H., Bertani, P., and Bechinger, B. (2006) A spectroscopic study of the membrane interaction of the antimicrobial peptide Pleurocidin. *Mol. Membr. Biol.* 23, 185–194.